Letters

Analysis and Design of a Cost-Effective WPT System With Single-Input and Multioutput Based on Buck-Integrated Rectifier

Xinghong He, Chenyan Zhu, Jin Tao, Yiming Zhang, and Ruikun Mai, *Senior Member, IEEE*

***Abstract*—Recently, wireless power transfer (WPT) has been a competitive power supply mode due to its convenience and safety. Normally, a WPT system provides only one output, whereas some devices request multiple voltage levels. In this letter, a single-input and multioutput WPT system is proposed. By integrating two buck converters into a full-wave rectifier, three constant voltage outputs are achieved with only four MOSFETs and two inductors. Besides, all MOSFETs can achieve zero voltage switching by designing the inductors. A 324-W prototype is fabricated with three voltage levels, i.e., 48, 24, and 18 V. Experimental results demonstrate that the three outputs are independent of loads and each other, and the overall efficiency ranges from 91.84% to 93.33%.**

***Index Terms*—Integrated rectifier, single-input and multioutput (SIMO), wireless power transfer (WPT).**

I. Introduction

WIRELESS power transfer (WPT) is capable of supplying power through the magnetic or electric field without an electrical connection. It has the technical advantage of being safe, convenient, and reliable compared to the traditional cable power supply method. Therefore, WPT technology is becoming more and more desirable in the fields of consumer electronics, electric vehicles, etc. [1], [2]. Usually, electrical equipment has not only the main power system but also the control system, and their voltage levels are various. Hence, it is imperative to implement WPT to power devices with multiple voltage levels.

A simple and common way of implementing multiple voltage outputs is adopting the multiple transmitters' and receivers' structure to achieve multi-input and multioutput [3]. However, additional transmitters and receivers would increase the volume of the system and make it complex.

Manuscript received 22 May 2023; revised 28 June 2023; accepted 17 July 2023. Date of publication 21 July 2023; date of current version 1 September 2023. This work was supported in part by the National Natural Science Foundation of China Joint Fund for Regional Innovation and Development under Grant U22A20222, in part by the Natural Science Foundation of Hebei Province under Grant E202105047, and in part by the National Natural Science Foundation of China under Grant 51977184. *(Corresponding author: Ruikun Mai.)*

The authors are with the School of Electrical Engineering, Southwest Jiaotong University, Chengdu 611756, China (e-mail: hxh@my.swjtu.edu.cn; zcy@my.swjtu.edu.cn; jhin1214@163.com; zhangym170011@outlook.com; mairk@swjtu.edu.cn).

Color versions of one or more figures in this article are available at https://doi.org/10.1109/TPEL.2023.3297712.

Digital Object Identifier 10.1109/TPEL.2023.3297712

In order to simplify the system and reduce volume, a single-input and multioutput (SIMO) structure with one transmitter and multireceivers is proposed [4]. However, the outputs will be disturbed by the presence of magnetic field cross-coupling between the receivers. Therefore, a coaxial dual receiver structure with a decoupled circuit is proposed, which utilizes a passive component connected with two receivers to cancel out the cross-coupling between each other [5]. Unfortunately, the cross-coupling is difficult to be accurately eliminated by the capacitor, and the circuit is complicated when the multireceiver structure is employed.

Compared to the multireceiver structure, the system with one transmitter and one receiver is further streamlined. One approach to achieve multiple outputs is to connect multiple double-T resonant circuits to a common port at the secondary side [6]. Whereas, a large number of passive components is required, which increases the volume of the system. Besides, the resonant conditions are complicated to satisfy. Therefore, dc–dc converters are adopted to achieve multiple outputs since the voltage regulations are easy to realize according to the requests [7]. Although the output voltage has a high degree of freedom, a large number of switches in the system increases the cost and volume of the system. A dual individually adjustable output WPT system without a dc–dc converter is proposed [8]. The secondary rectification circuit only uses two diodes and two MOSFETs, which can greatly reduce the cost. But this method is not suitable for a common ground system. To further improve the performance of the SIMO WPT system, Li et al. [9] have proposed a feasible solution that uses two half-wave rectifiers and asynchronous rectifiers to achieve multiple outputs to realize multiple outputs. However, a large number of semiconductor devices increase the cost of the system, and still, the power supply system cannot share the same ground.

In this letter, a cost-effective WPT system with SIMO based on a buck-integrated rectifier is proposed, which can achieve three load-independent outputs. The proposed structure implements the functions of a full-wave rectifier and two buck converters using only four switches. And the output voltages share common ground, which is more suitable for most power supply systems. The contributions and advantages of this letter can be summarized as follows.

1) Cost-Effective: In the proposed system, *LCC*-S resonant circuit is adopted, and only one transmitter and one

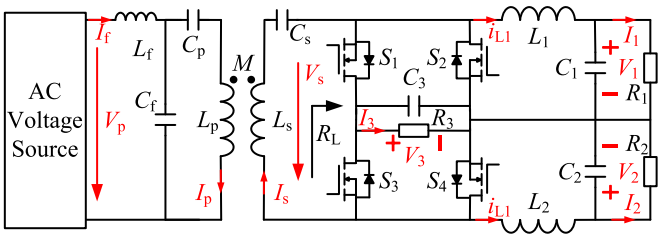

Fig. 1. Circuit structure of the proposed SIMO WPT system.

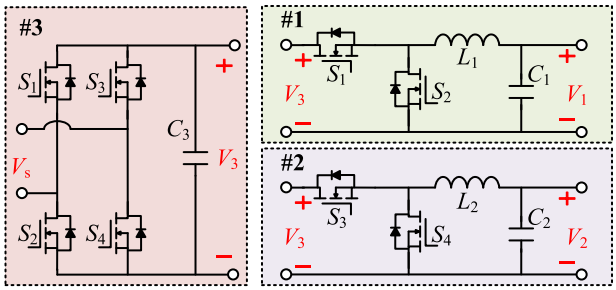

Fig. 2. Three-channel output composition of the proposed SIMO WPT system.

receiver are utilized. By employing the buck-integrated rectifier, three load-independent output voltages are achieved, requiring only four MOSFETs and two inductors.

2) Wide Applicability: In order to mitigate the potential impact of common mode noises on the system, most multiple-voltage-level requested systems are typically designed with the same ground. Therefore, the buck-integrated rectifier with three distinct output voltage levels is proposed, which has wide applicability due to the shared ground configuration.
3) Zero Voltage Switching (ZVS): In this letter, ZVS conditions for MOSFETs of the buck-integrated rectifier are analyzed, which is under the effect of inductor currents. By designing the output inductors of the rectifier, all MOSFETs in the proposed buck-integrated rectifier can achieve ZVS.

II. Proposed SIMO WPT System

A. Circuit Configuration

The circuit structure of the proposed SIMO WPT system is shown in Fig. 1. The primary *LCC* resonant network is composed of inductor L_f and capacitor C_f, C_p. V_p is the input voltage and I_f is the input current. $L_p(L_s)$ is the self-inductance of the transmitter (receiver), where the current is $I_p(I_s)$. M represents mutual inductance. C_s is the secondary resonant capacitor. S_1, S_2, and output inductor L_1 (S_3, S_4, and inductor L_2) form the buck converter of Channel #1 (Channel #2). Meanwhile, S_1, S_2, S_3, and S_4 consist of the active rectifier as Channel #3. C_1, C_2, and C_3 are filter capacitors. R_1, R_2, and R_3 are the dc loads for Channels #1, #2, and #3, respectively. The schematic diagram of the circuit structure of each of the channels is shown in Fig. 2.

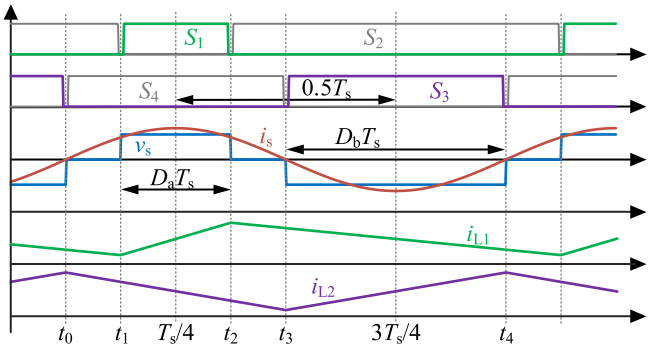

Fig. 3. Key waveforms of the proposed SIMO WPT system.

The resonant state of the circuit should satisfy the following equation:

$$\omega = 1/\sqrt{L_f C_f} = 1/\sqrt{(L_p - L_f)C_p} = 1/\sqrt{L_s C_s} \quad (1)$$

where ω represents the operating angular frequency of the circuit, which is defined as $\omega = 2\pi f_s$. f_s is the operating frequency of the system. According to Kirchhoff's voltage law, the voltage loop equation of the system can be derived as

$$\begin{bmatrix} 0 & j/(\omega C_f) & 0 \\ j/(\omega C_f) & 0 & -j\omega M \\ 0 & -j\omega M & R_{ac} \end{bmatrix} \begin{bmatrix} I_f \\ I_p \\ I_s \end{bmatrix} = \begin{bmatrix} V_p \\ 0 \\ 0 \end{bmatrix} \quad (2)$$

where R_{ac} is the equivalent load on the ac side. By solving (2), the ac output voltage V_s can be expressed as

$$V_s = \omega^2 C_f M V_p. \quad (3)$$

According to (3), the ac output voltage V_s is independent of the load and only related to mutual inductance M and input voltage V_p when the circuit parameters are determined.

B. Operational Principles

Fig. 3 shows the key waveforms of the proposed SIMO WPT system. D_a and D_b are the duty cycle of S_1 and S_3, respectively. The center of S_1 and S_3 is always $\pi(0.5T_s)$ apart. Besides, $S_1(S_3)$ is always complementary to $S_2(S_4)$. t_0 is set to be a reference ($t_0 = 0$), the four moments $t_1 - t_4$ can be calculated as

$$\begin{cases} t_1 = T_s/4 - D_a T_s/2 \\ t_2 = T_s/4 + D_a T_s/2 \\ t_3 = 3T_s/4 - D_b T_s/2 \\ t_4 = 3T_s/4 + D_b T_s/2 \end{cases}. \quad (4)$$

As shown in Fig. 2, output channel #3 is full-bridge rectified. According to Fourier analysis, the ratio K_s between V_s and the output dc voltage V_3 can be derived as

$$K_s = V_s/V_3 = \sqrt{2}\left[\sin(D_a\pi) + \sin(D_b\pi)\right]/\pi. \quad (5)$$

Output channels #1 and #2 are converted from output channel #3 by two buck converters, respectively. And the relationship between the output dc voltages V_3, V_2, and V_1 can be expressed as

$$\begin{cases} V_1 = D_a V_3 \\ V_2 = D_b V_3 \end{cases}. \quad (6)$$

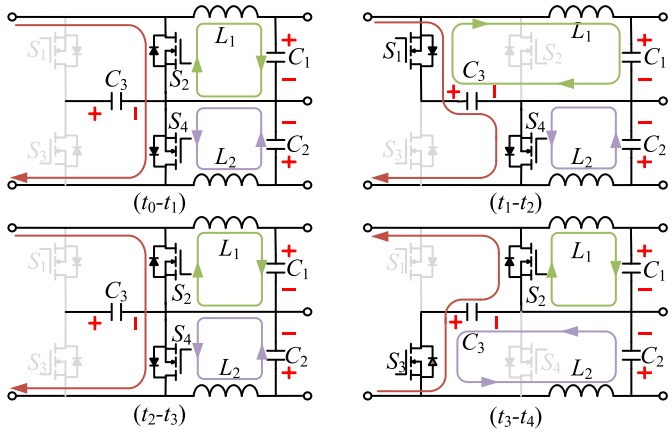

Fig. 4. Four operating states of the proposed SIMO WPT system.

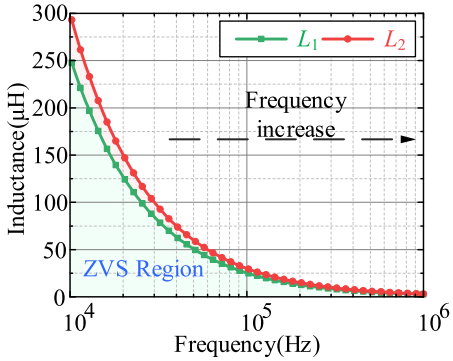

Fig. 5. Inductor versus frequency curves.

According to the energy conservation law, the equation can be obtained as

$$V_{\mathrm{s}}^2/R_{\mathrm{ac}} = V_1^2/R_1 + V_2^2/R_2 + V_3^2/R_3. \tag{7}$$

Substituting (5) and (6) into (7), R_{ac} can be derived as

$$R_{\mathrm{ac}} = K_{\mathrm{s}}^2/\left(D_{\mathrm{a}}^2/R_1 + D_{\mathrm{b}}^2/R_2 + 1/R_3\right). \tag{8}$$

Then, the time domain expression of the receiver current i_{s} can be obtained as

$$i_{\mathrm{s}}(t) = \sqrt{2}\frac{\omega^2 C_{\mathrm{f}} M V_{\mathrm{p}}\left(D_{\mathrm{a}}^2/R_1 + D_{\mathrm{b}}^2/R_2 + 1/R_3\right)}{K_{\mathrm{s}}^2}\sin(\omega t). \tag{9}$$

The output voltages can be calculated as follows:

$$\begin{cases} V_1 = D_{\mathrm{a}}\omega^2 C_{\mathrm{f}} M V_{\mathrm{p}}/K_{\mathrm{s}} \\ V_2 = D_{\mathrm{b}}\omega^2 C_{\mathrm{f}} M V_{\mathrm{p}}/K_{\mathrm{s}} \\ V_3 = \omega^2 C_{\mathrm{f}} M V_{\mathrm{p}}/K_{\mathrm{s}} \end{cases}. \tag{10}$$

According to (10), V_1, V_2, and V_3 are independent of the load. Meanwhile, by configuring the parameters of the system, the system can realize three various voltage outputs.

Fig. 4 shows the four operating states of the proposed SIMO WPT system.

Stage 1 (t_0-t_1): S_2 and S_4 are ON, S_1 and S_3 are OFF. The currents in inductors L_1 and L_2 decrease, and the inductors release energy.

Stage 2 (t_1-t_2): S_1 and S_4 are ON, S_2 and S_3 are OFF. The current in inductor L_1 increases, and L_1 stores energy. The current in inductor L_2 decreases, and L_2 releases energy.

Stage 3 (t_2-t_3): S_2 and S_4 are ON, S_1 and S_3 are OFF. The currents in inductors L_1 and L_2 decrease, and the inductors release energy.

Stage 4 (t_3-t_4): S_2 and S_3 are ON, S_1 and S_4 are OFF. The current in inductor L_1 decreases, and L_1 releases energy. The current in inductor L_2 increases, and L_2 stores energy.

III. Design of System Parameters

A. Design of Output Inductors

It should be noted that in the proposed buck-integrated rectifier, the value of the inductor will influence the currents through MOSFETs, which subsequently determine the achievement of ZVS for MOSFETs. The time-domain expressions for output inductors currents i_{L1} and i_{L2} in one period can be derived as

$$\begin{aligned} i_{\mathrm{L1}}(t) &= \begin{cases} V_1/R_1 + (V_3 - V_1)(t - T_{\mathrm{s}}/4)/L_1 & t \in [t_1, t_2) \\ V_1/R_1 - V_1(t - 3T_{\mathrm{s}}/4)/L_1 & t \in [t_2, t_1 + T_{\mathrm{s}}] \end{cases} \\ i_{\mathrm{L2}}(t) &= \begin{cases} V_2/R_2 - V_2(t - T_{\mathrm{s}}/4)/L_2 & t \in [t_0, t_3) \\ V_2/R_2 + (V_3 - V_2)(t - 3T_{\mathrm{s}}/4)/L_2 & t \in [t_3, t_4] \end{cases}. \end{aligned} \tag{11}$$

Then, the turn-ON currents $i_{\mathrm{sw1}}, i_{\mathrm{sw2}}, i_{\mathrm{sw3}}$, and i_{sw4} of the MOSFETs S_1, S_2, S_3, and S_4 can be calculated as

$$\begin{cases} i_{\mathrm{sw1}} = \sqrt{2} I_{\mathrm{s}} \cos(D_{\mathrm{a}}\pi) - [V_1/R_1 - (1 - D_{\mathrm{a}})V_1/(2L_1 f_{\mathrm{s}})] \\ i_{\mathrm{sw2}} = \sqrt{2} I_{\mathrm{s}} \cos(D_{\mathrm{a}}\pi) - [V_1/R_1 + (1 - D_{\mathrm{a}})V_1/(2L_1 f_{\mathrm{s}})] \\ i_{\mathrm{sw3}} = \sqrt{2} I_{\mathrm{s}} \cos(D_{\mathrm{b}}\pi) - [V_2/R_2 - (1 - D_{\mathrm{b}})V_2/(2L_2 f_{\mathrm{s}})] \\ i_{\mathrm{sw4}} = \sqrt{2} I_{\mathrm{s}} \cos(D_{\mathrm{b}}\pi) - [V_2/R_2 + (1 - D_{\mathrm{b}})V_2/(2L_2 f_{\mathrm{s}})] \end{cases}. \tag{12}$$

To achieve ZVS, the turn-ON currents of MOSFETs should satisfy the following equation [10]:

$$i_{\mathrm{sw1}} > 0, i_{\mathrm{sw2}} < 0, i_{\mathrm{sw3}} > 0, i_{\mathrm{sw4}} < 0. \tag{13}$$

By substituting (12) into (13), the inductor L_1, L_2 versus frequency curves are obtained.

For example, when the output channels are 48 V (9.6 Ω), 24 V (12 Ω), and 18 V (9 Ω), respectively, the values of the inductors L_1 and L_2 versus frequency are shown in Fig. 5. To make all MOSFETs can achieve ZVS, the values of the inductors should be below the curves. It should be pointed out that excessively small inductor values should be avoided, as they will result in large current ripples, consequently decreasing the efficiency.

B. Power Losses Analysis and Frequency Optimization

For the proposed system, there are four parts of losses, namely inverter losses (P_{INV}), WPT losses (P_{WPT}), rectifier losses (P_{REC}), and output inductor losses (P_{L}). Since the *LC*

TABLE I
ELECTRICAL PARAMETERS OF THE WPT SYSTEM

Symbol	Value	Symbol	Value	Symbol	Value
V_p	100 V	L_1	13.6 μH	R_{L1}	11 mΩ
M	15.9 μH	L_2	13 μH	R_{L2}	11 mΩ
C_f	110.6 nF	L_f	31.2 μH	R_f	18 mΩ
C_p	143.4 nF	L_p	55.9 μH	R_p	62 mΩ
C_s	63 nF	L_s	55.5 μH	R_s	63 mΩ
V_1	18 V	V_2	24 V	V_3	48 V
R_1	9 Ω	R_2	12 Ω	R_3	9.6 Ω

resonant circuits are the filters, only the fundamental harmonic is considered.

According to Li et al. [11], P_{INV} and P_{REC} mainly consist of switching losses and conduction losses. For the inverter, the switching losses can be ignored since the input zero phase angle is achieved. For the rectifier, the turn-ON losses are zero since ZVS is achieved. Therefore, P_{INV} and P_{REC} can be calculated as

$$P_{\mathrm{INV}} = 2I_{\mathrm{f}}^2 R_{\mathrm{con}}$$

$$P_{\mathrm{REC}} = V_3 f_{\mathrm{s}} \left[\frac{e_{\mathrm{OFF}}}{V_{\mathrm{R}} I_{\mathrm{R}}} + \frac{Q_{\mathrm{RR}}}{I_{\mathrm{RD}}}\right] \sum_{n=1}^{4} i_{\mathrm{sw}n} + \frac{1}{T_{\mathrm{s}}} \int_0^{T_{\mathrm{s}}} \left\{[i_{\mathrm{s}}(t) - i_{\mathrm{L1}}(t)]^2 + [i_{\mathrm{s}}(t) - i_{\mathrm{L2}}(t)]^2\right\}^2 \times R_{\mathrm{con}} dt \quad (14)$$

where R_{con} is drain-source on-state resistance, e_{OFF} is the turn-OFF energy losses of MOSFETs under reference voltage (V_{R}) and current (I_{R}). And Q_{RR} and I_{RD} are the reverse recovery charge and the reference current of the diode, respectively.

The main losses in WPT are determined by inductors resistances, which can be represented as

$$P_{\mathrm{WPT}} = I_{\mathrm{f}}^2 R_{\mathrm{f}} + I_{\mathrm{p}}^2 R_{\mathrm{p}} + I_{\mathrm{s}}^2 R_{\mathrm{s}} \quad (15)$$

where R_{f}, R_{p}, and R_{s} are the internal resistance of L_{f}, L_{p}, and L_{s}, respectively. I_{f}, I_{p}, and I_{s} can be calculated by (2). Due to the skin effect, the ac internal resistance of the litz-wire increases with frequency. And the ac-to-dc winding resistance ratio F_{RLMF} of litz-wire can be expressed as [12]

$$F_{\mathrm{RLMF}} = 1 + \pi^5 \left(5N_{\mathrm{ll}}^2 - 1\right) d_{\mathrm{str}}^6 \mu_0^2 f_{\mathrm{s}}^2 / \left(2880 {\rho_\omega}^2 p^2\right) \quad (16)$$

where N_{ll} is the number of winding layers and sublayers, and d_{str} is the optimum conductor strand diameter for windings conducting sinusoidal. μ_0 is free space permeability. ρ_ω is conductor resistivity, and p is the distance between center of the wires/strands in the inductor layer and sublayer. It is observed from (16), with augmenting frequency, the resistances of the inductors will increase when the other parameters are determined.

The last part, output inductor losses P_{L}, can be expressed as

$$P_{\mathrm{L}} = \left[\int_0^{T_{\mathrm{s}}} i_{\mathrm{L1}}(t)^2 R_{\mathrm{L1}} dt \cdot + \int_0^{T_{\mathrm{s}}} i_{\mathrm{L2}}(t)^2 R_{\mathrm{L2}} dt\right] / T_{\mathrm{s}} \quad (17)$$

where $R_{L1}$and R_{L2} are the resistance of the output inductors.

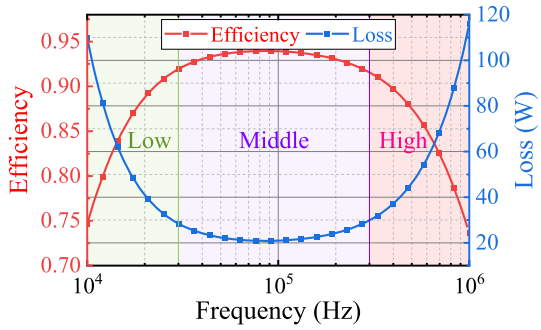

Fig. 6. Efficiency curves calculated at different frequencies.

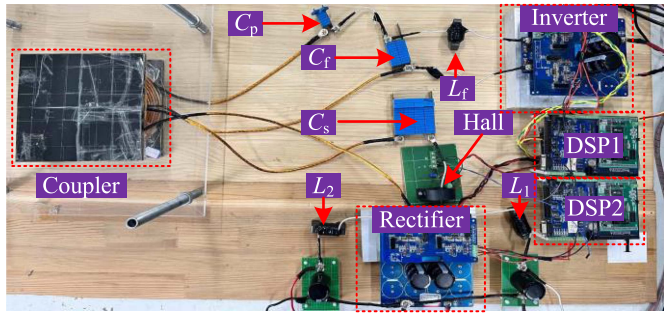

Fig. 7. Experimental platform of the proposed SIMO WPT system.

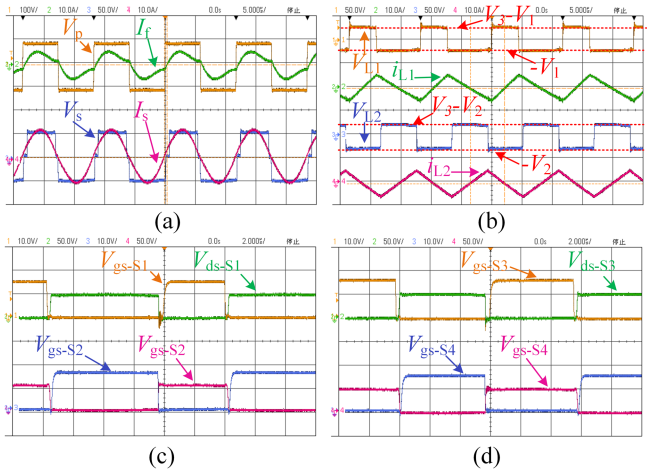

Fig. 8. Experimental waveform with rated outputs. (a) Output of the inverter and input of the rectifier. (b) Voltages and currents of the output inductors L_1 and L_2. (c) ZVS of S_1 and S_2. (d) ZVS of S_3 and S_4.

Therefore, the total loss of the system is the sum of four parts, which can be calculated as

$$P_{\mathrm{Loss}} = P_{\mathrm{INV}} + P_{\mathrm{WPT}} + P_{\mathrm{REC}} + P_{\mathrm{L}}. \quad (18)$$

Table I illustrates the actual parameters of the system designed for 85 kHz. With the parameters listed in Table I, the system efficiency and power loss as a function of frequency are calculated, as depicted in Fig. 6. It can be found that the optimal frequency range for the proposed SIMO WPT system is between 30 and 300 kHz.

TABLE II
COMPARISON BETWEEN THE REFERENCES [6], [7], [8], [9] AND THIS WORK

Ref	Method	Original configuration				Three output channels with the same methods		
		Output channels	Additional passive components	Semiconductor devices on the receiver side	Efficiency (%)	Output channels	Additional passive components	Semiconductor devices on the receiver side
[6]	Multiple Double-T Resonant Circuits	2	12	8 diodes	91.1	3	18	12 diodes
[7]	Multiple dc–dc converters	3	3	4 diodes + 8 MOSFETs	85		3	4 diodes + 8 MOSFETs
[8]	Rectifier with Two half-wave Channels	2	0	2 diodes + 2 MOSFETs	90.9		0	3 diodes + 3 MOSFETs
[9]	Rectifier with Two half-wave Channels and One Full-wave channel	3	0	2 diodes + 6 MOSFETs	90.6		0	2 diodes + 6 MOSFETs
This work	Buck-integrated Rectifier	3	2	4 MOSFETs	93.3		2	4 MOSFETs

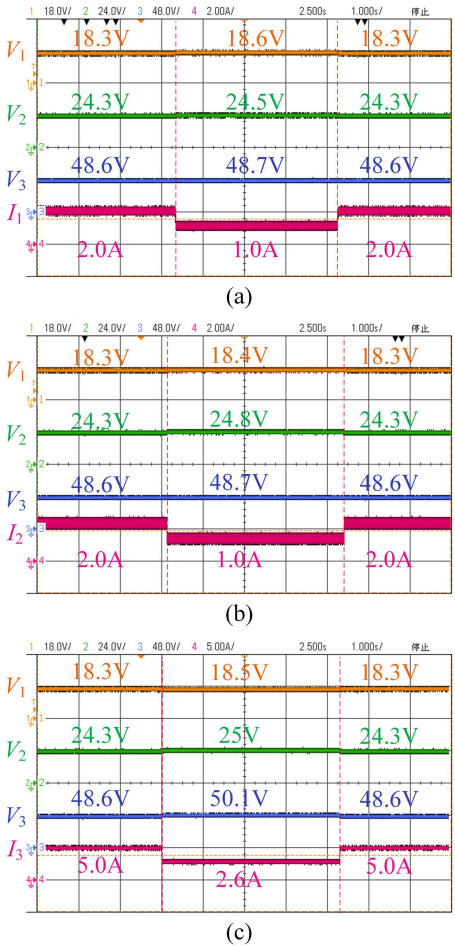

Fig. 9. System output waveforms when one of the loads varies. (a) When R_1 changes from 9 to 18 Ω. (b) When R_2 changes from 12 to 24 Ω. (c) When R_3 changes from 9.6 to 19.2 Ω.

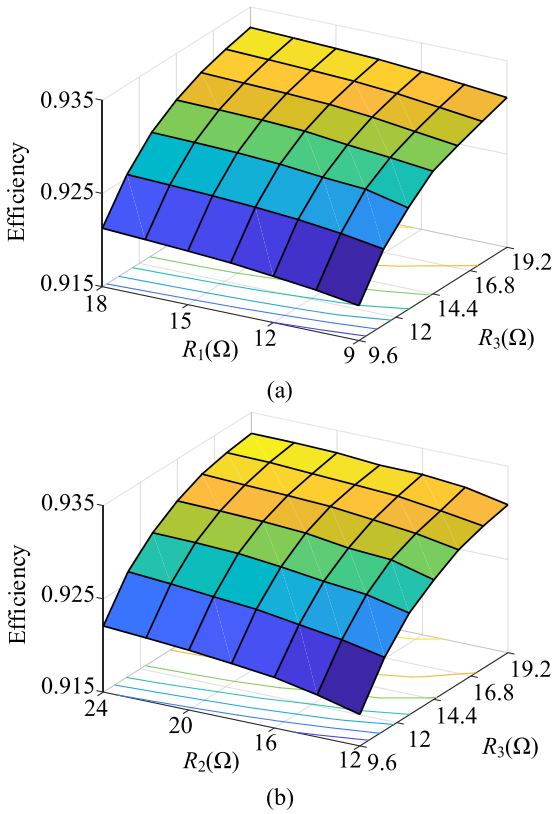

Fig. 10. Experimental efficiencies. (a) Versus R_1 and R_3. (b) Versus R_2 and R_3.

IV. EXPERIMENTAL VERIFICATION

To verify the feasibility of the proposed system, a 324-W prototype operating at 85 kHz has been built, as shown in Fig. 7. The experimental parameters are shown in Table I.

Fig. 8 shows the experimental waveforms under the rated power of the system. Fig. 8(a) depicts the output of the inverter and input of the rectifier, and Fig. 8(b) illustrates the voltages and currents of the output inductors L_1 and L_2. And the experimental waveforms of the switching state are exhibited in Fig. 8(c) and (d), where it can be observed that all four MOSFETs can achieve ZVS.

Fig. 9(a) shows the output waveforms when $R_2 = 12\,\Omega$, $R_3 = 9.6\,\Omega$, and R_1 varies from 9 to 18 Ω. The voltage fluctuation rates of V_1, V_2, and V_3 are 1.67%, 0.83%, and 0.21%, respectively. Fig. 9(b) shows the output waveforms when $R_1 = 9\,\Omega$, $R_3 = 9.6\,\Omega$, and R_2 changes from 12 to 24 Ω. The voltage fluctuation rates of V_1, V_2, and V_3 are 0.55%, 2.1%, and 0.21%, respectively. Fig. 9(c) shows the output waveforms when $R_1 = 9\,\Omega$, $R_2 = 12\,\Omega$, and R_3 ranges from 9.6 to 19.2 Ω. The voltage fluctuation rates of V_1, V_2, and V_3 are 1.11%, 2.92%, and 3.13%, respectively.

Fig. 10(a) shows the system efficiency when $R_2 = 12\,\Omega$, R_1 varies from 9 to $18\,\Omega$, and R_3 varies from 9.6 to $19.2\,\Omega$, respectively, which ranges from 93.28% to 91.87%. Fig. 10(b) shows the system efficiency when $R_1 = 9\,\Omega$, R_2 varies from 12 to $24\,\Omega$, and R_3 varies from 9.6 to $19.2\,\Omega$, respectively, which ranges from 93.33% to 91.84%. The overall efficiency ranges from 91.84% to 93.33%.

Table II shows the comparison between this work and others' work in terms of original output channels, number of additional passive components, semiconductor devices on the secondary side, and system efficiency. It should be noted that the additional passive components are connected after the receiver compensate networks. It can be found that, though the proposed method has two small additional output inductors, the least semiconductor devices. To compare more fairly, the number of passive components and semiconductor devices with three output channels by various methods are also listed. Still, the proposed method has the least semiconductor devices. Therefore, the proposed system has the advantage of low cost.

V. Conclusion

This letter presents a SIMO (WPT) system. Compared with the traditional SISO system, three load-independent output voltages are achieved, requiring no additional semiconductor devices but only two inductors. A 324-W laboratory prototype is fabricated with three voltage levels, i.e., 48, 24, and 18 V. Experiments have proved that when a single load varies, the voltage fluctuation of the other load is within 3.13%. All the MOSFETs in the proposed buck-integrated rectifier can achieve ZVS. The overall efficiency ranges from 91.84% to 93.33%.

References

[1] Z. Zhang, H. Pang, A. Georgiadis, and C. Cecati, "Wireless power transfer—An overview," *IEEE Trans. Ind. Electron.*, vol. 66, no. 2, pp. 1044–1058, Feb. 2019.

[2] Y. Chen, S. He, B. Yang, S. Chen, Z. He, and R. Mai, "Reconfigurable rectifier-based detuned series-series compensated IPT system for anti-misalignment and efficiency improvement," *IEEE Trans. Power Electron.*, vol. 38, no. 2, pp. 2720–2729, Feb. 2023.

[3] M. Q. Nguyen, Y. Chou, D. Plesa, S. Rao, and J.-C. Chiao, "Multiple-inputs and multiple-outputs wireless power combining and delivering systems," *IEEE Trans. Power Electron.*, vol. 30, no. 11, pp. 6254–6263, Nov. 2015.

[4] L. Sun, H. Tang, and S. Zhong, "Load-independent output voltage analysis of multiple-receiver wireless power transfer system," *IEEE Antennas Wireless Propag. Lett.*, vol. 15, pp. 1238–1241, 2016.

[5] R. Mai, Y. Luo, B. Yang, Y. Song, S. Liu, and Z. He, "Decoupling circuit for automated guided vehicles IPT charging systems with dual receivers," *IEEE Trans. Power Electron.*, vol. 35, no. 7, pp. 6652–6657, Jul. 2020.

[6] Y. Li, J. Hu, X. Li, and K.-W. E. Cheng, "A flexible load-independent multi-output wireless power transfer system based on cascaded double T-resonant circuits: Analysis, design and experimental verification," *IEEE Trans. Circuits Syst. I, Reg. Papers*, vol. 66, no. 7, pp. 2803–2812, Jul. 2019.

[7] M. McDonough, "Integration of inductively coupled power transfer and hybrid energy storage system: A multiport power electronics interface for battery-powered electric vehicles," *IEEE Trans. Power Electron.*, vol. 30, no. 11, pp. 6423–6433, Nov. 2015.

[8] C. Zhu et al., "Analysis and design of cost-effective WPT systems with dual independently regulatable outputs for automatic guided vehicles," *IEEE Trans. Power Electron.*, vol. 36, no. 6, pp. 6183–6187, Jun. 2021.

[9] X. Li, F. Zheng, H. Wang, X. Dai, Y. Sun, and J. Hu, "Analysis and design of a cost-effective single-input and regulatable multioutput WPT system," *IEEE Trans. Power Electron.*, vol. 38, no. 6, pp. 6939–6944, Jun. 2023.

[10] X. Zhang et al., "A control strategy for efficiency optimization and wide ZVS operation range in bidirectional inductive power transfer system," *IEEE Trans. Ind. Electron.*, vol. 66, no. 8, pp. 5958–5969, Aug. 2019.

[11] Y. Li et al., "Extension of ZVS region of series–series WPT systems by an auxiliary variable inductor for improving efficiency," *IEEE Trans. Power Electron.*, vol. 36, no. 7, pp. 7513–7525, Jul. 2021.

[12] R. P. Wojda and M. K. Kazimierczuk, "Winding resistance and power loss of inductors with litz and solid-round wires," *IEEE Trans. Ind. Appl.*, vol. 54, no. 4, pp. 3548–3557, Jul./Aug. 2018.